Nanoscale

Accepted Manuscript

This article can be cited before page numbers have been issued, to do this please use: A. Mahata, I. Choudhuri and B. Pathak, *Nanoscale*, 2015, DOI: 10.1039/C5NR01575H.

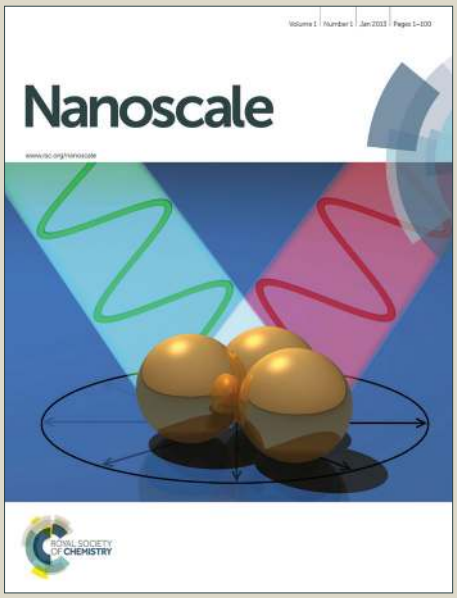

ROYAL SOCIETY OF CHEMISTRY

www.rsc.org/nanoscale

View Article Online
DOI: 10.1039/C5NR01575H

Cuboctahedral Platinum (Pt_{79}) Nanocluster Enclosed by Well Defined Facets Favours the Di-sigma Adsorption and Improves the Reaction Kinetics for Methanol Fuel Cell

Arup Mahata,[†] Indrani Choudhuri, [†] Biswarup Pathak, [†,#,*]

[†]Discipline of Chemistry, School of Basic Sciences, Indian Institute of Technology (IIT) Indore, Indore, M.P., India

[#]Center for Material Science and Engineering, Indian Institute of Technology (IIT) Indore, Indore, M. P., India

Email: biswarup@iiti.ac.in

Abstract

The methanol dehydrogenation steps are studied very systematically on the (111) facet of cuboctahedral platinum (Pt_{79}) nanocluster enclosed by well-defined facets. The various intermediates formed during the methanol decompositions are adsorbed at the edge and bridge site of the facet either vertically (through C- and O-centre) or parallely. The di-sigma adsorption (parallely) on the (111) facet of the nanocluster is the most stable structure for most of the intermediates and such binding improves the interaction between the substrate and the nanocluster thus the catalytic activity. The reaction thermodynamics, activation barrier, and temperature dependent reaction rates are calculated for all the successive methanol dehydrogenation steps to understand the methanol decomposition mechanism and these values are compared with previous studies to understand the catalytic activity of such nanocluster. We find the catalytic activity of the nanocluster is excellent while comparing with any previous reports and the methanol dehydrogenation thermodynamics and kinetics are best when the intermediates are adsorbed in a di-sigma manner.

Keywords: Methanol Fuel Cell, di-sigma, cuboctahedral, Nanocluster, dehydrogenation

View Article Online
DOI: 10.1039/C5NR01575H

1. Introduction

The ever-increasing demand of energy and the problems associated with fossil fuel burning is the primary reason of searching for various alternative energy sources. Fuel cells are efficient and non-polluting energy sources due to their high energy densities and wide operating range of temperature compared to other conventional systems[1-5]. Direct methanol fuel cells (DMFCs) are very promising over any other kind of fuel cells due to their low operating temperature, ease of handling and high energy density and wide variety of portable applications[6-8]. The adsorption and catalytic dehydrogenation of methanol on the catalyst surface is a crucial step in DMFC. The chemisorption and decomposition of methanol on electrode's surfaces have been widely studied in recent years. However, the dehydrogenation mechanism of methanol over electrode's surface is not fully understood. As there are three different types of bond (C-H, O-H and C-O) present in methanol, the complexity of the dehydrogenation process arises whether the bond scission occurs via C-H, O-H or C-O bonds. To understand the underlying reaction mechanism of methanol decomposition on catalyst's surface, extensive studies (experimental and theoretical) have been carried out by various research groups[9-22]. These experimental and theoretical studies on methanol decomposition concludes that the C-O bond scission is not a favourable one but the sequence of O-H and C-H bond activations steps are very crucial and could be the rate determining steps to improve the efficiency of the methanol fuel cell. Apart from the initial dehydrogenation through C-H or O-H bonds, the surface morphology and size of the metal nanoparticles also plays an important role in the bond scission process which in turn governs the catalytic activity of the metal catalyst. In this context, metal nanoclusters surrounded by multiple numbers of well-defined facets show its potential in comparison to their bulk metal surfaces. Metal nanoclusters enclosed by multiple numbers of facets are very noble types of catalyst and found to be very promising in different electro-oxidation reaction[21, 23] due to the

View Article Online
DOI: 10.1039/C5NR01575H

presence of high surface unsaturation. Such unsaturation serves as a highly active site for activating chemical bonds which in turn controls the catalytic activity. Many theoretical studies are done on small size metal nano-cluster[18,24] to understand the catalytic activity of the nanocluster. However, the size of the nanocluster is very important to its catalytic reactivity due to their finite-size effects[25-30]. These low-coordinated sites have higher d-band energies, which actually increase the reactivity of these sites[31-32]. But, to the best of our knowledge, there are no reports on methanol decomposition on the well-defined facets of platinum nano-cluster. The role of different types of binding sites and modes of the substrate-adsorbent is yet to be known. Therefore, to understand the activity of the nano-sized catalyst and the whole decomposition process over such nanocluster's surfaces, it is necessary to model nano-cluster surrounded by different type of facets. The nanocluster with cuboctahedral shape is one of the stable forms due to its high symmetry. Hence we have modelled a ~1 nm size cubocahedral platinum nanocluster enclosed by well-defined low index facets to understand the methanol decomposition pathway. Some questions and comparisons will arise whether the adsorption behaviour and reaction energy of the nanocluster's surfaces is similar to the bulk surfaces or not? Similarly, whether the rate determining steps and the reaction mechanism are similar as in the bulk surfaces or not? In this study, an attempt has been made to address these questions by comparing with previously reported results. The highly unsaturated binding sites such as edge vs. bridge site of the nanocluster surface is considered for the methanol decomposition to get the maximum catalytic activity.

The (111), (002) and/or (200) planes are mainly observed in the XRD patterns of experimentally synthesized Pt nanocluster[33-37]. As the (200)/(002) has the same pattern as in (100)/(001), we have considered cubooctahedral Pt79 cluster with (111) and (001) facet to model the real experimental situation. Here cuboctahedral Pt_{79} cluster is modelled with eight

View Article Online
DOI: 10.1039/C5NR01575H

(111) and six (001) facets (Fig. 1a) to improve the catalytic activity of the surfaces. We have considered various active sites on the (111) facet of the nanocluster for our methanol dehydrogenation study as platinum (111) surface is the most exposed and stable surface. The edge position (Fig. 1), formed by the intersection of the (111) facets, is considered to be one of the highly unsaturated active site of the cluster. Two more highly active catalytic sites such as bridge and three fold hollow sites (Fig. 1) are also considered on the (111) facet of the nanocluster. Here we have considered methanol dehydrogenation proceeds via adsorption of the various intermediates on the (111) facet of the nanocluster via C- and O- centre.

Therefore, the complete dehydrogenation pathway is studied considering three kind of adsorption (*) to the edge, bridge and hollow site (Fig. 1) of the (111) facet. All the intermediates adsorbed at the edge position are mentioned as vertical adsorption via C- or O-centre. Similarly, the intermediates adsorbed at the bridge site of the (111) facet of the nanocluster mentioned as parallel adsorption via di-sigma manner [Figure 1b]. Some other adsorbents are minima at the three-fold hollow site of the (111) facet. The binding preferences on the edge, bridge or the hollow site of the (111) facet are accessed based on their relative stabilities. The relative stabilities of the adsorbed intermediates in the different binding sites are discussed in the supporting information (Table S1 & Scheme S3).

2. Computational Methods and Models

The first-principles calculations are performed using projected augmented wave (PAW) method[38], as implemented in the Vienna ab initio simulation package (VASP).[39] The exchange-correlation interaction is treated in the level of the GGA using Perdew-Burke-Ernzerhof (GGA-PBE).[40] A 22×22×22 $Å^3$ cubic supercell is used to optimize the structures of

View Article Online
DOI: 10.1039/C5NR01575H

the metal clusters to rule out the possibility of interaction of periodically repeated metal clusters. The Brillouin zone is sampled using gamma k-point (1×1×1). We have increased the k-points to 2×2×2 for the Pt_{79} cluster and total energy improved by 0.002 eV. As the box size is quite high therefore we continue our calculation with gamma point only. All the atoms are relaxed for the full structural relaxation. The climbing nudged elastic band (CI-NEB) method[41] is used to locate the transition states. Six intermediate images are used in each CI-NEB pathway. Vibrational frequencies for the initial, transition and final states of the reactions are calculated and transition states are confirmed by the presence of one imaginary frequency. Zero-point energy (ZPE) is calculated as ZPE $=\sum_i 1/2h\upsilon_i$ where h is Planck's constant and υ_i is the frequency of the i^{th} vibrational mode. The adsorption energies (E_{ad}) for all possible adsorbates are calculated using the following equation.

$$E_{ad} = E_{cluster\text{-}molecule} - (E_{cluster} + E_{molecule})$$

where $E_{cluster\text{-}molecule}$, $E_{cluster}$ and $E_{molecule}$ are the energies of the adsorbed species on cluster, the platinum cluster and the corresponding molecular species. The reaction energy (enthalpy) is calculated using the total energy difference between the products and the reactants. Thus negative reaction energy suggests the exothermic nature of the reaction whereas positive reaction energy suggests the endothermic nature of the reaction. Activation barrier are calculated by the energy difference between the transition and the initial state. The reaction energy and activation barrier is calculated with zero point energy (ZPE) correction and entropy contribution but we have tabulated without ZPE and entropy contribution so that vis-à-vis comparison can be made with previous theoretical studies. However, the ZPE and entropy corrected activation barrier has been given in the supporting information (Scheme S2). The ZPE correction and entropy contribution is included for activation free energy calculation for temperature dependent rate constant.

View Article Online
DOI: 10.1039/C5NR01575H

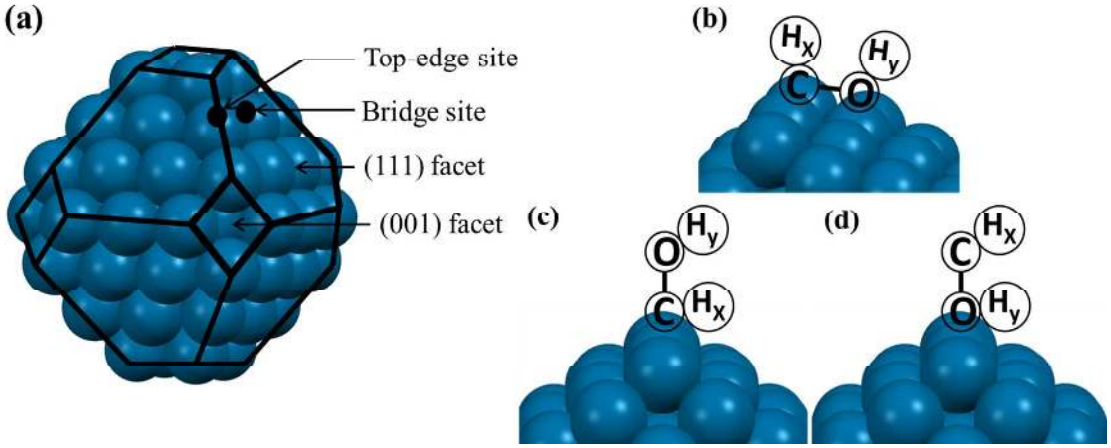

Figure 1. (a) Cuboctahedral Pt_{79} nanocluster enclosed by fourteen facets. Intermediates adsorb in a (b) di-sigma fashion and at the top edge site via (c) C- and (d) O-centre

3. Results and Discussion

The results and discussion part is divided into four sections for the successive dehydrogenation of four methanol hydrogens. The various intermediates involved for the first (CH_2OH, CH_3O), second (CHOH, CH_2O), third (CHO, COH) and fourth methanol dehydrogenation (CO) steps are discussed as following.

In the beginning of each step, we have discussed the adsorption type, relative stabilities, and adsorption energy of all the intermediates involved for their respective dehydrogenation steps. The intermediates are studied at the three active sites (edge, bridge and hollow) adsorbed through C- and O-atoms. The reaction energy and C-/O-H bond activation barriers for each of those processes are calculated and discussed in their respective sections to understand their reaction thermodynamics. At the end of each section, our calculated results are compared with the available experimental and theoretical data to understand and compare the catalytic activity of our model system.

View Article Online
DOI: 10.1039/C5NR01575H

From here on, methanol, methoxy, hydroxymethyl, hydroxymethelene, formaldehyde, formyl, hydroxymethylidyne, carbon monoxide represented as *CH_3OH, *CH_3O, *CH_2OH, *CHOH, *CH_2O, *CHO, *COH, and *CO when adsorbed through C-atom and *$OHCH_3$, *OCH_3, *$OHCH_2$, *OHCH, *OCH_2, *OCH, *OHC, *OC when adsorbed through O-atom. Similar convention used for the bridge structures (*CH_3OH, *CH_3O etc.) as used for the intermediates adsorbed through C-centre at edge position.

3.1. First Dehydrogenation Step:

Here we have studied the first dehydrogenation mechanism of the methanol which will lead to the formation of hydroxymethyl (*CH_2OH) or methoxy (*CH_3O) intermediates. So in the beginning, we have discussed about the adsorption behaviour, adsorption energy and relative energetics of all the intermediates (methanol, hydroxymethyl, and methoxy) involved in the first dehydrogenation step and then discussed about their reaction thermodynamics and activation barrier for each of these (C-H/O-H) bond dissociation process on the nanocluster's surface.

3.1.1. Adsorption Type and Energetics:

Methanol (*CH_3OH): The dehydrogenation process of methanol starts with its adsorption on the nanocluster's (111) surface. The methanol molecule calculated to be a minima at the top edge position adsorbed as *CH_3OH (Fig. 2a) and *$OHCH_3$ (Fig. 2b) with adsorption energy of -0.24, -0.38 eV respectively. The other structure (Fig. 2c) calculated to be a minimum is the one adsorbed at the bridge site with adsorption energy of -0.19 eV. Their relative energetic study shows that *$OHCH_3$ is the most stable structure when adsorbed through O-centre and stable by 0.18 and 0.19 eV than the CH_3OH adsorbed at the edge and bridge position respectively. The Pt-C and Pt-O distances at the top edge position adsorbed as *CH_3OH and *$OHCH_3$ structures are 3.24 Å and 2.52 Å respectively but at the bridge

View Article Online
DOI: 10.1039/C5NR01575H

position, *CH_3OH adsorbed via di-sigma manner where methanol interacts weakly with the nanocluster surface through the C-H bond. In the bridge structure, the Pt-H, Pt-C and Pt-O bond distances are 2.83 Å, 3.32 Å and 3.59 Å respectively (Fig. 2c). Such structural parameters reflect that the methanol molecule interacting weakly with the nanocluster's sruface. Interestingly, our relative energetic study shows methanol adsorbed at the top edge site (through C-atom) and bridge site are equally stable though methanol interacts weakly with the nanocluster while adsorbed at the bridge position.

Shustorovich [42] reported that saturated molecules prefer to bind at the top position of the metal surface, thus agreeing well with our results. The C-O-H bond angle of the methanol changes from 107.72º to 109.34º after adsorption through O-atom, indicating that there is an interaction between the methanol oxygen and platinum of the nanocluster. Slab model surface calculations showed that methanol adsorption is most favourable when it binds through O-atom on the top edge site of Pt(111) surface. Mavrikakis et al. showed that methanol weakly adsorbs through O-atom with adsorption energy of -0.33 eV [22].

In our calculation, the optimized Pt-O bond distance is of 2.52 Å which is in close agreement with the Pt-O bond distance of 2.59Å [19] reported previously. The cluster model calculation by Ishikawa and Goddard et al. reported that methanol binds weakly to the top site of platinum through O-atom with binding energy of -0.66 eV [18] and -0.64 eV [24] respectively. Higher adsorption value is due to the different size of clusters (Pt_{10} and Pt_8) used for their model study. Experimentally, methanol reported to be adsorbed weakly at the top site of Pt(111) through O-atom [8-9,27] with binding energy of ~-0.40-0.50 eV [9,13]. Our calculated results also suggest that methanol binds weakly to the cluster and among the different binding sites of the cluster, methanol binds most strongly at the top edge site

View Article Online
DOI: 10.1039/C5NR01575H

through O-atom with adsorption energy of -0.38 eV, thus supporting the trend of previous experimental and theoretical results.

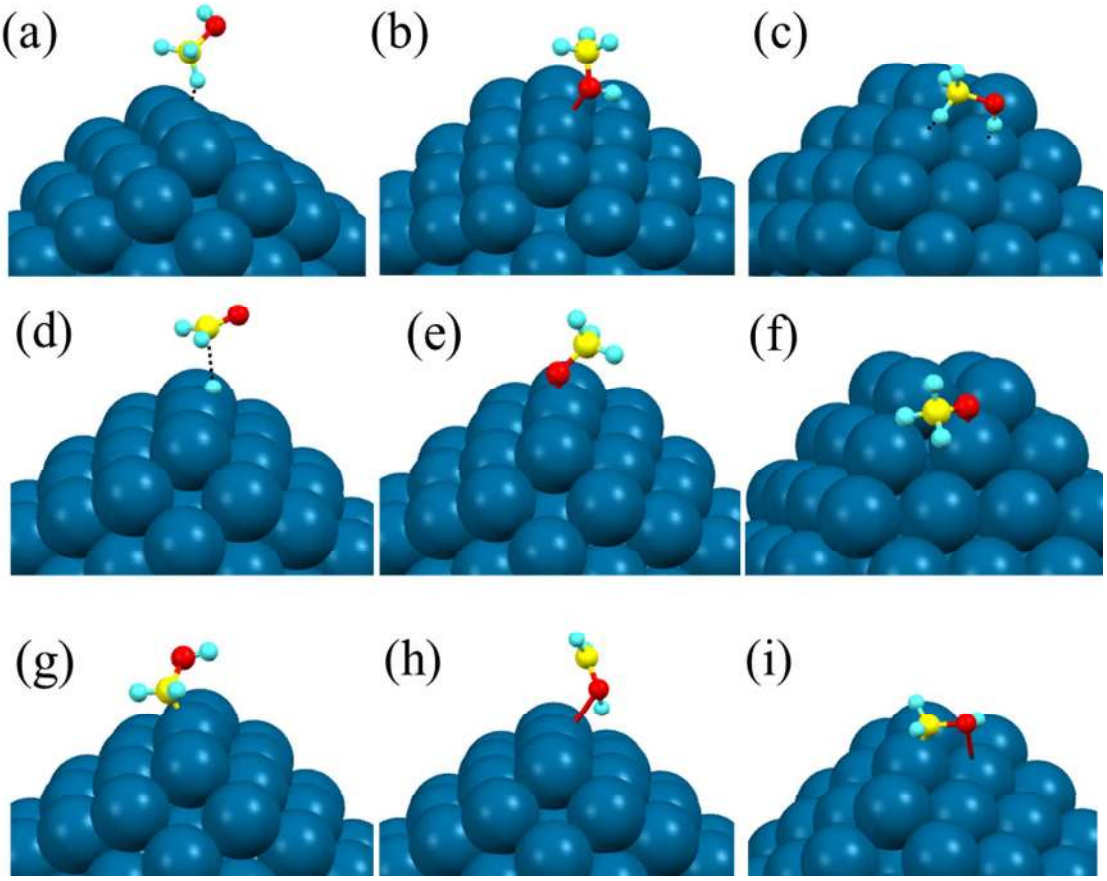

Figure 2: Adsorbed methanol at edge via (a) C-atom and (b) O-atom; (c) bridge position. Methoxy at edge via (d) C-atom and (e) O-atom; (f) bridge position. Hydroxymethyl at edge via (g) C-atom and (h) O-atom; (i) bridge position.

Methoxy (*CH_3O): Methoxy is an important intermediate during methanol dehydrogenation process. *OCH_3 is formed through the O-H bond scission of *$OHCH_3$ with adsorption energy of -2.47 eV. In the adsorbed *OCH_3 structure (Fig. 2e), the Pt-O bond distance (1.97 Å) is shorter than the Pt-O (2.52 Å) bond distance in methanol. The CH_3O structure calculated to be a minima where one of the C-H bond strongly interacting with the nanocluster with C-H bond length of 2.15 Å (Fig. 2d). *CH_3O binds at the bridge-site in a di-sigma manner with

View Article Online
DOI: 10.1039/C5NR01575H

adsorption energy of -2.25 eV. In this di-sigma manner, one hydrogen atom of $–CH_3$ oriented to the nanocluster, forming Pt-H, Pt-C and Pt-O bond distances of 2.09 Å, 2.99 Å and 2.01 Å respectively (Fig. 2f). Therefore, we find the adsorption energy is higher by 0.22 eV at the top edge position than at the bridge position, which is also reflected from the Pt-O bond distances at the edge (1.97 Å) and the bridge (2.01 Å) position respectively. Relative energetic study shows, $*OCH_3$ at the top edge site is energetically more stable by 0.30 eV than $*CH_3O$ at the bridge site. Both bond distances and relative energetics suggest about the favourable binding of $*OCH_3$ over $*CH_3O$. Interestingly, both at the bridge and edge position, methyl group interact weakly with the nanocluster. In slab model calculation, Mavrikakis et al.[17] showed that methoxy binds through oxygen at the top position with Pt-O distance of 2.03 Å and adsorption energy of -1.54 eV while Desai et al.[19] reported that methoxy binds through oxygen at the bridge position with average Pt-O distances of 2.51 Å and adsorption energy of -1.66 eV. Recently, Kramer et al.[43] also suggested about the top-site binding of methoxy through oxygen atom with the adsorption energy of -1.59 eV. Goddard et al. also suggested the binding of methoxy at the top site with adsorption energy of -1.07 eV[24] on Pt_8 cluster. Ishikawa et al.[18] obtained site preference for methoxy in a three-fold hollow site with the binding energy of -2.07 eV in their cluster model study. Though there are many studies on the favourable binding site of the methoxy group but most of them reported that methoxy binds through the O-atom, which agrees well with our calculated results.

Hydroxymethyl ($*CH_2OH$): We find $*CH_2OH$ binds at the top edge position with adsorption energy of -2.76 eV and Pt-C bond distance of 2.08 Å (Fig. 2g). It even binds weakly as $*OHCH_2$, where O-atom bridging between the two platinum centres with Pt-O bond distances of 3.70 Å and 3.10 Å (Fig. 2h) and adsorption energy of -1.07 eV. Longer Pt-O bond distances show their reluctance of binding through the O-atom. At the top edge

View Article Online
DOI: 10.1039/C5NR01575H

position, *CH_2OH (Fig. 2i) structure is more stable by 1.55 eV than *$OHCH_2$, suggesting its preference of binding through C-atom. Our findings are well in agreement with the extended Huckel calculation by Hoffman et al.[44] that unsaturated radical species such as carbon in hydroxymethyl will certainly form a covalent bond with the metal of the cluster's surface. The *CH_2OH adsorption on Pt(111) surface reported by various groups and their calculated adsorption energy values are -1.98 eV[17], -2.17 eV[19], and -2.08 eV[43] while adsorbed at the top Pt site through C-atom. Cluster model calculations reported higher adsorption energy of -2.51 eV[18] and -2.85 eV[24] for the similar type of geometries. Therefore, previous studies on slab and cluster models support our findings and our calculated value of adsorption energy agrees well with the cluster model study.

3.1.2 Reaction Thermodynamics:

In this part, methanol dehydrogenation energetics related to the formation of methoxy and hydroxymethyl has been discussed. We have calculated the reaction energy and activation barrier for the following possible elementary steps based on their adsorption behaviour.

*$CH_3OH \rightarrow$ *CH_2OH+*H (1) *$OHCH_3 \rightarrow$ *$OHCH_2$+*H (1a)

*$CH_3OH \rightarrow$ *CH_3O+*H (2) *$OHCH_3 \rightarrow$ *OCH_3+*H (2a)

Table 1: Reaction energy (eV) and activation barrier (eV) for the following elementary steps (1-2 and 1a-2a) while adsorbed vertically through C- and O-atom and parallely at the bridge site.

Elementary Reactions	Edge				[1]Bridge	
	[1]C-bonded		[2]O-bonded			
	Reaction Energy	Activation Barrier	Reaction Energy	Activation Barrier	Reaction Energy	Activation Barrier
[1] $CH_3OH \rightarrow CH_2OH$+H [2] $OHCH_3 \rightarrow OHCH_2$+H	-0.57	0.31	1.36	1.38	-0.29	0.29

View Article Online
DOI: 10.1039/C5NR01575H

[1] $CH_3OH \rightarrow CH_3O+H$ [2] $OHCH_3 \rightarrow OCH_3+H$	0.47	0.64	0.29	0.62	0.41	0.65

C-H bond activation

Edge vs. bridge site:

At the edge position, the C-H bond activation from $*CH_3OH$ to the formation of $*CH_2OH$ calculated to be exothermic by -0.57 eV (step 1) and endothermic by 1.36 eV (step 1a) if the intermediates ($*CH_3OH$ and $*OHCH_2$) are adsorbed at the top edge position through C and O-centre respectively. The calculated activation barriers are 0.31 eV and 1.38 eV respectively. Therefore, the C-H bond activation is favourable at the edge position when the intermediate is adsorbed through C-centre.

At the bridge position, C-H bond dissociation for the formation of $*CH_2OH$ calculated to be exothermic by -0.29 eV (step 1) and the activation barrier is of 0.29 eV. Therefore, the C-H bond activation barrier of methanol at the bridge position (0.29 eV) is lower and very much comparable with the top edge site (0.31 eV) when adsorbed through C-centre.

It is clear from the reaction energies and activation barriers that C-H bond activation is very much favourable at the bridge position while the intermediates are adsorbed in a di-sigma manner. It is also clear that C-H bond activation is very much favourable when methanol adsorbed through C-atom ($*CH_3OH$) than through O-atom ($*OHCH_3$). Recently Kramer et al.[43] reported that the activation barrier for this process is of 0.55 eV when it binds through C-atom. Greeley et al.[22] reported the activation barrier of 0.67 eV for the C-H bond activation of methanol when it binds through C-atom. Cluster model study by Ishikawa et al.[18] showed the activation barrier of 0.42 eV for C-H activation process when adsorbed through C-atom. Therefore, in all the previous studies the C-H bond activation barrier reported to be lowest

View Article Online
DOI: 10.1039/C5NR01575H

when the intermediates are adsorbed though carbon atom but we report the C-H bond activation barrier is the lowest (0.29 eV) when the intermediates are adsorbed in a di-sigma manner.

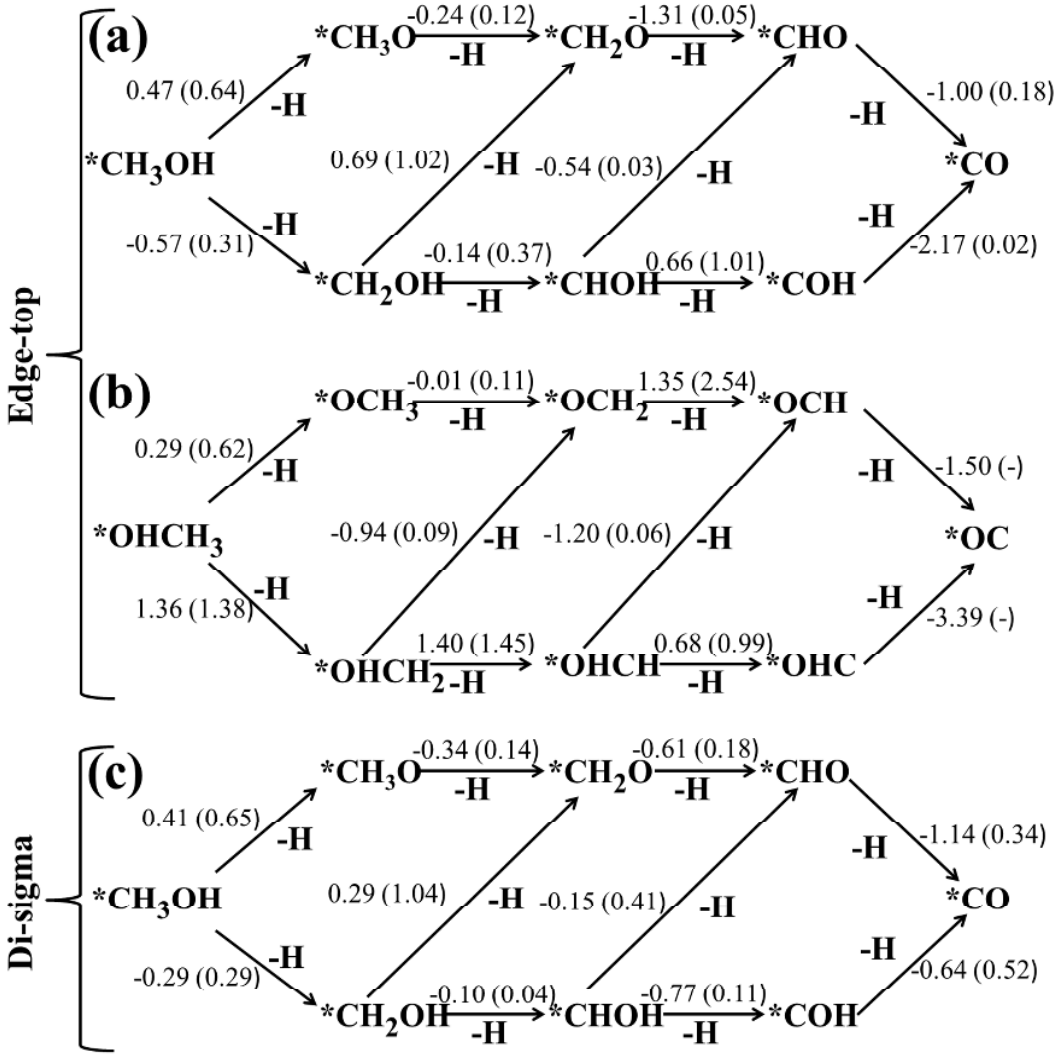

Scheme 1: The reaction energies (eV) and activation barriers (eV, values in parenthesis) for the successive methanol dehydrogenation at different binding sites (a) adsorbed through C-atom and (b) O-atom at top edge position and (c) bridge position.

View Article Online
DOI: 10.1039/C5NR01575H

O-H bond activation:

Edge vs. bridge site:

The O-H bond dissociation is endothermic by 0.29 eV (step 2) and 0.47 eV when adsorbed through O- and C-centre respectively (Step 2-2a). The activation barriers for these two processes are 0.62 eV and 0.64 eV respectively.

The reaction (step 2) is endothermic by 0.41 eV and the calculated activation barrier is of 0.65 eV while adsorbed in a di-sigma manner. Interestingly, the O-H bond activation barriers are very much comparable whether the intermediates are adsorbed through O- (0.62 eV), C centre (0.64 eV) or in a di-sigma (0.65 eV) manner.

C-H vs. O-H bond activation:

Our reaction thermodynamics and activation barrier study shows C-H bond activation is very much favourable over O-H bond activation at the catalysts surface. Such C-H bond activation preferences over O-H bond activation can be explained from the following findings.

Firstly, the produced $*CH_2OH$ binds more strongly than $*CH_3O$ intermediates at the bridge and edge positions respectively. Secondly, the C-H bond energies are lower than the O-H bond energies. The calculated gas phase reaction energy for the C-H bond activation is 3.98 eV whereas O-H bond activation is 4.23 eV, suggesting that C-H activation is more favourable over O-H activation (Scheme S1; Supporting Information). In fact the adsorption behaviour of $*CH_3OH$ also suggests its preference for dehydrogenation through C-H bond activation as one of the methanol carbon hydrogen (C-H = 1.13 Å) orients towards the surface of the nanocluster and interacts strongly.

The preference of C-H bond activation over O-H activation, to form $*CH_2OH$ is reported in the literature using Pt(111) surface and cluster model study. Sanket et al. [19]

View Article Online
DOI: 10.1039/C5NR01575H

showed that C-H bond activation is exothermic by -0.16 eV whereas O-H bond activation is endothermic by 0.66 eV over Pt (111) surfaces. Mavrikakis et al.[22] reported the activation barrier of 0.81 eV for O-H bond activation and 0.67 eV for C-H bond activation. Kramer, Cui-Yu and Desai et. al. reported O-H bond activation barrier on Pt (111) surfaces is of 0.81 eV[43], 0.85 eV[20], and 1.47 eV[19] respectively. Ishikawa et al.[18] in their cluster model study reported that the formation of hydroxymethyl (activation energy 0.42 eV) is more favourable than the methoxy formation (activation energy 0.77 eV).

Therefore, our calculations show the same trend as reported on Pt(111) surfaces and platinum cluster model study that C-H bond activation is more favourable than the O-H bond activation. Here also, we find our calculated activation barrier is the lowest (0.29 eV) while comparing with all the values reported previously. Therefore we assume such Pt cub-octahedral nanocluster could be an excellent catalysis for C-H bond activation.

On the other hand, when intermediates are adsorbed through O-atom, O-H bond activation (barrier = 0.62 eV) is favourable over C-H bond activation (barrier = 1.38 eV) due to the stronger adsorption of $*OCH_3$ (adsorption energy = -2.47 eV) than $*OHCH_2$ (adsorption energy = -1.07 eV). In fact their relative energetic study also shows $*OCH_3$ intermediate is more stable (by 1.04 eV) than $*OHCH_2$.

3.2. Second Dehydrogenation Step:

In this step, we have studied the second successive dehydrogenation step of methanol which lead to the formation of hydroxymethelene (*CHOH) and formaldehyde ($*CH_2O$) intermediates.

View Article Online
DOI: 10.1039/C5NR01575H

3.2.1 Adsorption Type and Energetics:

Hydroxymethelene (*CHOH): We find *CHOH (Fig. 3a), is stable at the top edge position with adsorption energy of -3.67 eV whereas *OHCH binds weakly at the same site with adsorption energy of -0.25 eV (Fig. 3b). The Pt-C and Pt-O bond distances are 1.89Å and 2.72Å in case of *CHOH and *OHCH intermediates respectively. *CHOH intermediate calculated to be more stable by 3.03 eV than the *OHCH intermediate. Both adsorption energy and relative energy study shows *CHOH intermediate is the most preferred. *CHOH adsorbed intermediate calculated to be stable at the bridge position too with adsorption energy of -4.86 eV, in a di-sigma manner with Pt-C and Pt-O bond distances of 2.03Å and 2.72Å respectively (Fig. 3c). The *CHOH structure is 0.15 eV more stable in the bridge position than *CHOH at the top edge position. As *CHOH has a divalent C-atom, it is expected to be stable at the bridge position to fulfil its covalency (become tetravalent), thus favouring the bridged structure.

Slab model study reported that *CHOH binds with equal adsorption energy in the top and bridge position of the Pt(111) surface with adsorption energy of -3.24 eV[17]. A recent study[43] on Pt(111) surface shows that it prefers to bind at the bridge position with binding energy -3.39 eV. However, study on cluster surface shows that *CHOH is stable at the top position with adsorption energy of -3.79 eV which is in close agreement with our calculated adsorption energy (-3.67 eV) of *CHOH at the top edge position[18]. Another cluster model calculation[24] shows that it is most preferred at the bridge position with adsorption energy of -3.68 eV but our calculated adsorption value is maximum (4.86 eV) when adsorbed in a di-sigma manner.

View Article Online
DOI: 10.1039/C5NR01575H

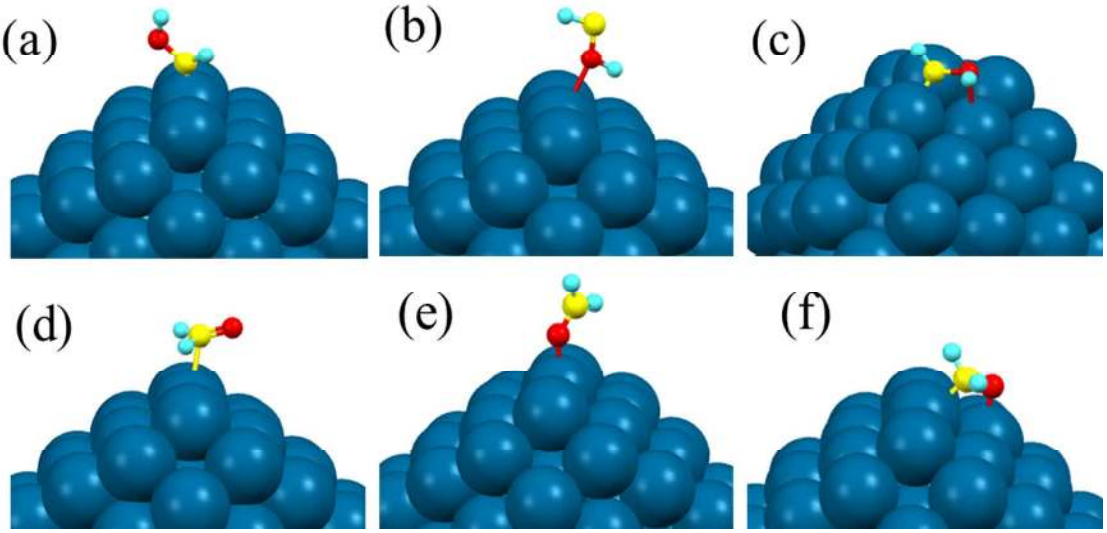

Figure 3: Adsorbed hydroxymethelene at edge via (a) C-atom and (b) O-atom; (c) bridge position. Formaldehyde at edge via (d) C-atom and (e) O-atom; (f) bridge position.

Formaldehyde (*CH_2O):

We find *CH_2O is also most stable when it adsorbed in a di-sigma manner, at the bridge position (Fig. 3f) with binding energy of -1.94 eV. Here, the Pt-O and Pt-C bond distances are 2.05Å and 2.11Å respectively. In case of edge position, OCH_2 binds strongly with the nanocluster with adsorption energy of -0.55 eV (Fig. 3e), where as *CH_2O binds weakly with adsorption energy -0.17 eV (Fig. 3d). The Pt-C and Pt-O bond distances are 2.67 Å and 2.18 Å in case of *CH_2O and *OCH_2 respectively. The bridge *CH_2O intermediate is energetically most stable by 0.37 eV and 0.10 eV than adsorbed through C and O-centre respectively. Higher adsorption value of *CH_2O at the bridge position (adsorption energy -1.94 eV) than edge position (adsorption energy -0.17 eV) is due to the CO group of formaldehyde interacting more strongly with the surface of the nanocluster. This is more clear from the C-O bond distance of 1.35Å, 1.22Å and 1.23Å for the bridge, top edge *CH_2O and *OCH intermediates respectively. So such bond elongation at the bridge site justifies about the charge transfer between the C-O group and the platinum nanocluster.

View Article Online
DOI: 10.1039/C5NR01575H

Slab model surface calculation[19] on Pt(111) showed that formaldehyde tend to bind at the bridge position in a di-bridge fashion with adsorption energy of -0.50 eV where the Pt-O and Pt-C bond lengths are of 2.12Å and 2.06Å respectively. Others slab model calculation also reported similar kind of binding behaviour with the adsorption energy of -0.43 eV[43] and -0.50 eV[17]. Cluster model calculation[24] also reported about the di-sigma bonding behaviour of formaldehyde with adsorption energy of -0.41 eV. Therefore our result such as di-sigma bonding preference of formaldehyde agrees well with previous reports.

3.2.2 Reaction Energy and Activation Barriers

In the second step, the formed methoxy (*CH_3O) and hydroxymethyl (*CH_2OH) intermediate can further undergo C-H and O-H bond activation. C-H bond activation on methoxy (*CH_3O) and hydroxymethyl (*CH_2OH) leads to the formation of formaldehyde (*CH_2O) and hydroxymethelene (*CHOH) intermediates respectively whereas hydroxymethyl (*CH_2OH) can undergo only O-H bond activation to form formaldehyde (*CH_2O). The possible elementary steps are shown as following (steps 3-5 and 3a-5a).

*CH_2OH→ *CHOH+*H (3) *$OHCH_2$→ *OHCH+*H (3a)

*CH_3O→ *CH_2O+*H (4) *OCH_3→ *OCH_2+*H (4a)

*CH_2OH→ *CH_2O+*H (5) *$OHCH_2$→ *OCH_2+*H (5a)

Table 2: Reaction energy (eV) and activation barrier (eV) for the following elementary steps (3-5 and 3a-5a) while adsorbed vertically through C- and O-atom and parallely at the bridge site.

View Article Online
DOI: 10.1039/C5NR01575H

Elementary Reactions	Edge				^{1}Bridge	
	^{1}C-bonded		^{2}O-bonded			
	Reaction Energy	Activation Barrier	Reaction Energy	Activation Barrier	Reaction Energy	Activation Barrier
$^{1}CH_2OH \rightarrow CHOH+H$ $^{2}OHCH_2 \rightarrow OHCH+H$	-0.14	0.37	1.40	1.45	-0.10	0.04
$^{1}CH_3O \rightarrow CH_2O+H$ $^{2}OCH_3 \rightarrow OCH_2+H$	-0.24	0.12	-0.01	0.11	-0.34	0.14
$^{1}CH_2OH \rightarrow CH_2O+H$ $^{2}OHCH_2 \rightarrow OCH_2+H$	0.69	1.02	-0.94	0.09	0.29	1.04

C-H bond activation

Edge vs. bridge site:

At the edge position, $*CH_2OH$ can undergo C-H bond activation to form *CHOH. The reaction (step 3) is calculated to be exothermic by -0.14 eV and endothermic by 1.40 eV when the intermediates are adsorbed through C (step 3) and O-centre (step 3a) respectively. The calculated activation barriers for the step 3 and 3a are 0.37 eV and 1.45 eV respectively.

Similarly, $*CH_3O$ can undergo C-H bond activation to form $*CH_2O$ (step 4) while adsorbed through C- and O-centre respectively. The reaction energy and activation barriers are calculated to be -0.24 eV and 0.12 eV for C-centre and -0.01 and 0.11 eV for O-centre respectively. Kramer et al.[43] reported the activation barrier of 0.19 eV for the $*OCH_2$ formation from $*OCH_3$, agrees well with our results.

On the other hand, at the bridge site, the C-H activation from $*CH_2OH$ (step 3) and $*CH_3O$ is exothermic by -0.10 eV and -0.34 eV respectively. The activation barriers for these

View Article Online
DOI: 10.1039/C5NR01575H

two steps are 0.04 eV and 0.14 eV respectively. Therefore, the C-H bond activation barrier is the lowest (0.04 eV) when intermediates adsorbed in a di-sigma manner.

Mavrikakis et al.[22] found the activation barrier of 0.25 eV for the decomposition of methoxy over Pt(111) surface. Cui-Yu et al.[20] found the activation barrier of 0.27 eV for the bridge position. Therefore our calculated activation barrier is far lower than what reported in the literature, shows the excellent catalytic activity of the Pt (111) facet of the nanocluster.

O-H bond activation

Edge vs. bridge site:

The O-H bond activation of $*CH_2OH$ (step 5-5a) calculated to be endothermic and exothermic by 0.69 eV and -0.94 eV when intermediates are adsorbed through C- and O-centre respectively. The activation barriers for these two steps are 1.02 eV (step 5) and 0.09 eV (step 5a) respectively. In case of adsorbed hydroxymethyl ($*CH_2OH$), hydroxyl group does not interact with the cluster, thus difficult for O-H bond dissociation, resulting in higher endothermicity (0.69 eV) and activation barrier (1.02 eV).

At the bridge site, the O-H bond activation of $*CH_2OH$ is endothermic by 0.29 eV and activation barrier for this process is of 1.04 eV. Therefore, the $*CH_2O$ formation at the bridge site is not favourable.

C-H vs. O-H bond activation:

It is clear from the activation barriers that at the edge and bridge position, *CHOH formation via C-H bond activation is more preferable than the $*CH_2O$ formation via O-H bond activation. Reaction energy values suggest the same trend. Interestingly, when it binds through oxygen atom, O-H bond activation (formation of $*OCH_2$) becomes more favourable over C-H bond activation (formation of *OHCH). This can be due to the following reasons.

View Article Online
DOI: 10.1039/C5NR01575H

Firstly, *CH_2OH adsorbs very strongly (-2.76 eV) than *$OHCH_2$ (-1.07 eV), thus favouring its dehydrogenation. Secondly, the O-H bond distance in the adsorbed *$OHCH_2$ is 1.01 Å, which is longer than in the gas-phase geometry (0.97 Å), showing its tendency to dehydrogenate via O-H bond activation. Therefore, such adsorption fashion favours the O-H bond activation over C-H bond activation. Furthermore, *OCH_2 is energetically more stable (by 0.27 eV) over *CH_2O.

However, the higher activation barrier of 1.38 eV for the first C-H bond activation of methanol to the formation of *$OHCH_2$ in the first dehydrogenation step (step 1a) might not allow further dehydrogenation to the formation of OCH_2 from $OHCH_2$ at this position in spite of its lower activation barrier (0.09 eV).

It is clear from the activation barriers of the first dehydrogenation steps (step 1-1a, 2-2a) and second dehydrogenation steps (step 3-3a, 4-4a, 5-5a) that *CH_3OH→ *CH_2OH→*CHOH is the most favourable path at the bridge position. But at the edge position, reaction is more favourable through *CH_3OH→*CH_2OH followed by *CH_3O→*CH_2O which is in agreement with the study of Desai et al. who reported that although methanol prefers to dehydrogenate via C-H bond activation forming hydroxymethyl but in the subsequent step methoxy intermediate prefers to form formaldehyde via C-H bond activation. In contrast, *$OHCH_3$→*OCH_3→*OCH_2 is the most favourable pathway when intermediates are adsorbed through O-atom.

View Article Online
DOI: 10.1039/C5NR01575H

3.3. Third Dehydrogenation Step:

Here, we have studied the dehydrogenation of the third hydrogen of methanol which lead to the formation of formyl (*CHO) and hydroxymethylidyne (*COH) intermediates from the formaldehyde (*CH_2O) and hydroxymethelene (*CHOH) intermediates.

3.3.1 Adsorption Type and Energetics:

Formyl (*CHO):

*CHO is adsorbed strongly in the edge position (Fig. 4a) with adsorption energy of -3.03 eV and Pt-C bond distance of 1.96 Å. In contrast, *OCH binds very weakly (Fig. 4b) with adsorption energy of -0.60 eV at the top edge position. In the bridge position, *CHO intermediate adsorbs in a di-sigma way (Fig. 4c) with adsorption energy of -3.47 eV. In the bridge position, Pt-C, Pt-O and C-O distances are 2.07Å, 2.15Å and 1.29 Å respectively. Elongation of C-O bond occurs from 1.22 Å to 1.29 Å, suggesting the change of hybridisation on the carbon centre. Surprisingly, *CHO intermediate calculated to be most stable at the edge position by 0.08 eV than the bridge position though the adsorption energy is higher at the bridge position.

Previously Kramer et al.[43] reported that formyl binds most preferably through C-atom at the top site of the Pt(111) surfaces, with adsorption energy of -2.29 eV whereas Desai et al.[19] reported that formyl prefers to adsorb in a di-sigma manner with the adsorption energy -2.45 eV. Gomes et al.[45] found that formyl adsorbed at the bridge site through C-atom with binding energy of -2.61 eV. Previous cluster model study reported the adsorption energy of -2.71 eV [24] and -2.84 eV [18] for the binding of formyl through C-atom on the top site of the nanocluster surface.

View Article Online
DOI: 10.1039/C5NR01575H

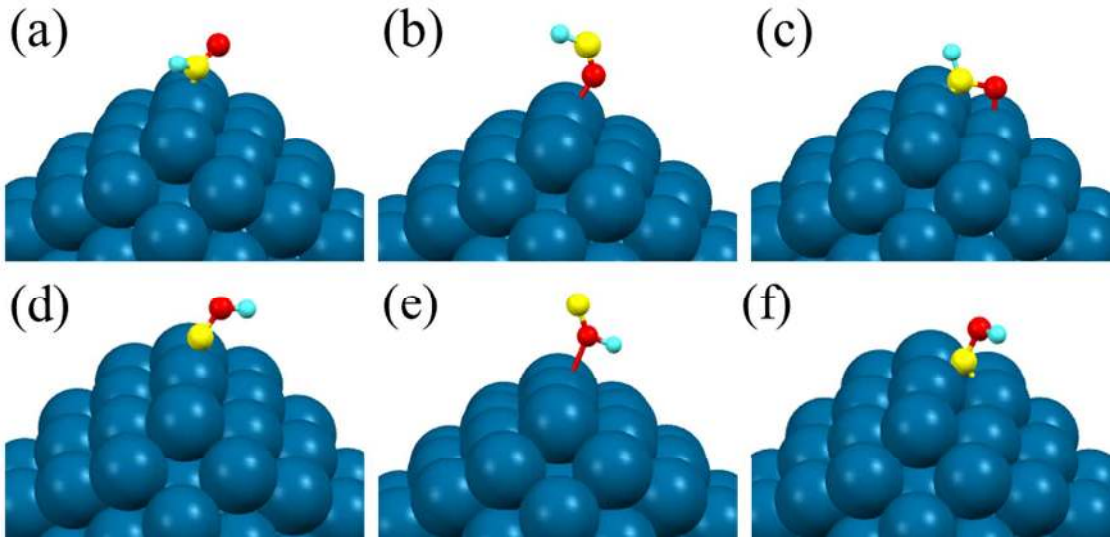

Figure 4: Adsorbed formyl at edge via (a) C-atom and (b) O-atom; (c) bridge position. Hydroxymethylidine at edge via (d) C-atom and (e) O-atom; (f) bridge position.

Hydroxymethylidyne (*COH):

In our study, hydroxymethylidyne adsorps at the top site of the edge position with adsorption energy of -3.94 eV and -0.63 eV for *COH (Fig. 4d) and *OHC (Fig. 4e) structures respectively. The Pt-C and Pt-O bond distances in these two structures are 1.78Å and 2.75Å respectively. The structure is not stable at the bridge position. On the other hand, the *COH calculated to be a minima at the hollow site of the Pt(111) facet with adsorption energy of -5.67 eV and Pt-C bond distances of 2.02Å (Fig. 4f) respectively. Interestingly, the intermediate is most stable at the hollow site (by 1.58 eV) than the edge site.

Slab model calculation by Kramer et al.[43] reported that COH preferably binds at the hollow site through C-atom with adsorption energy of -4.70 eV. Cluster model calculation by Goddard et al.[24] reported that COH prefers to bind at the hollow site through C-atom with binding energy of -5.25 eV. Another cluster model study by Ishikawa et al.[18] found strong

View Article Online
DOI: 10.1039/C5NR01575H

adsorption through C-atom with the adsorption energy of -3.05 eV and -4.86 eV at the top and hollow site respectively.

3.3.2. Reaction Energies and Activation Barriers

The formed formaldehyde and hydroxymethelene intermediate can further undergo C-H and O-H bond activation. C-H bond activation leads to the formation of formyl and hydroxymethylidyne from formaldehyde and hydroxymethelene respectively whereas only hydroxymethelene can undergo O-H bond activation to form formyl intermediate. The proposed elementary steps are given as following (steps 6-8 and 6a-8a).

*CHOH→ *COH+*H (6) *OHCH→ *OHC+*H (6a)

*CH_2O→ *CHO+*H (7) *OCH_2→ *OCH+*H (7a)

*CHOH→ *CHO+*H (8) *OHCH→ *OCH+*H (8a)

Table 3: Reaction energy (eV) and activation barrier (eV) for the following elementary steps (6-8 and 6a-8a) while adsorbed vertically through C- and O-atom and parallely at the bridge site.

Elementary Reactions	Edge				[1]Bridge	
	[1]C-bonded		[2]O-bonded			
	Reaction Energy	Activation Barrier	Reaction Energy	Activation Barrier	Reaction Energy	Activation Barrier
[1]CHOH→ COH+H [2]OHCH→ OHC+H	0.66	1.01	0.68	0.99	-0.77	0.11
[1]CH2O→ CHO+H [2]OCH2→ OCH+H	-1.31	0.05	1.35	2.54	-0.61	0.18
[1]CHOH→ CHO+H [2]OHCH→ OCH+H	-0.54	0.03	-1.20	0.06	-0.15	0.41

View Article Online
DOI: 10.1039/C5NR01575H

C-H bond activation

Edge vs. bridge site:

*CHOH can undergo C-H bond activation to form *COH (step 6) with activation energy barrier of 1.01 eV and 0.99 eV while adsorbed through C- and O-centre respectively (step 6-6a). The reaction energies for these process are 0.66 eV (step 6) and 0.68 eV (step 6a) respectively. Both reaction energy and activation barrier value suggests that this process is not favourable at edge position irrespective of their binding mode. Ishikawa et al. reported the activation barrier of 0.53 eV for this process when the intermediates were bonded through C-atom.

The C-H activation on the $*CH_2O$ intermediate (step 7) calculated to be exothermic by -1.31 eV with activation barrier of 0.05 eV. In contrast, when *OHC is formed from $*OCH_2$ (step 7a), the step becomes endothermic by 1.35 eV with the activation barrier of 2.54 eV. Therefore, the C-H activation on $*CH_2O$ is very much favourable when adsorbed through C-atom.

At the bridge position, on the other hand, *CHOH undergoes C-H bond activation to form *COH (step 6) with activation barrier of 0.11 eV. Reaction energy of this step is exothermic by -0.77 eV. $*CH_2O$ can also undergo C-H bond activation to form *CHO and the reaction is exothermic by -0.61 eV with activation barrier of 0.18 eV.

Therefore, the conversion of CHOH→COH is highly unfavourable at the edge position due to the high activation barrier whereas at the bridge position it is very much favourable. It is due to the different adsorption behaviour of the involved intermediates at the bridge position. At the bridge position, *COH adsorbs very strongly at the three-fold hollow site with the adsorption energy -5.67 eV, resulting the lower activation barrier for the process. For the same process, Kramer et al. reported the activation barrier of 0.56 eV.

View Article Online
DOI: 10.1039/C5NR01575H

O-H bond activation

Edge vs. bridge site:

The calculated O-H activation barrier for the formation of *CHO from *CHOH (step 8) intermediate is 0.03 eV and *OCH from *OHCH intermediate is 0.06 eV (step 8a). The reaction energies for these two process are -0.54 eV (step 8) and -1.20 eV (step 8a) respectively. Though the adsorption behaviour of *CHOH and *OHCH are different but activation energies are very much comparable for both the cases (step 8 and step 8a). This could be due to their comparable adsorption energies of the *CHO/*OCH intermediate and the *CHOH/*OHCH intermediate. Ishikawa et al. also reported the activation barrier of 0.44 eV for the same process when adsorbed through C-atom.

Rather at the bridge position, the activation barrier for the formation of *CHO from *CHOH is 0.41 eV and the reaction is exothermic by -0.15 eV. Activation barrier is high due to the strong adsorption behaviour (adsorption energy -4.86 eV) of *CHOH at the bridge position.

C-H vs. O-H bond activation:

It is clear from the calculated reaction energy and activation barrier values that C-H decomposition of *OCH_2 or *OHCH is not favoured when it binds through O-atom, due to the lower adsorption energy of the *OCH or *OHC intermediates. But the O-H bond activation step (Step 8a) is exothermic which could be due to the similarity in the adsorption behaviour of *OHCH (Fig 3b) and *OCH (Fig 4b) intermediates. The orientation of Trans *OHCH is similar with *OCH, resulting easy dehydrogenation from O-atom. Therefore its quite unlikely, the formation of *OHCH from *$OHCH_2$ intermediate due to high activation barrier 1.45 eV (step 3a), so the successive dehydrogenation steps from there on.

View Article Online
DOI: 10.1039/C5NR01575H

In case of *CHOH when adsorbed at the edge site, there are possibilities of formation of either *COH or *CHO through C-H or O-H bond activation respectively. Generally, the *COH formation is not favourable due to strong adsorption behaviour of *CHOH intermediate. However, this process is quite favourable at the bridge site with activation barrier of 0.11 eV, due to the very strong adsorption (-5.67 eV) behaviour of *COH at the three-fold hollow position. At the edge site, formation of *CHO becomes favourable either via O-H bond activation from *CHOH (step 8) or via C-H bond activation from *CH_2O (step 7). The C-H bond activation from *CH_2O intermediate calculated to exothermic (-1.31 eV) with low (0.05 eV, step 7) activation barrier.

At the bridge position, *CH_3OH→ *CH_2OH→*CHOH is the most favourable pathway up to second dehydrogenation step. The calculated activation barrier of third dehydrogenation step shows that the reaction proceeds via *CH_3OH→ *CH_2OH→ *CHOH→ *COH pathway. At the edge position, reaction proceed through *CH_3OH→*CH_2OH followed by *CH_3O→ *CH_2O→ *CHO.

3.4. Fourth Dehydrogenation Step

In this step, dehydrogenation pathways for the formation of carbon monoxide from the formyl and hydroxymethyl intermediates are discussed.

3.4.1 Adsorption Type and Energetics:

Carbon monoxide (*CO) and Hydrogen: The adsorption of carbon monoxide has been widely studied experimentally as well theoretically over Pt(111) surfaces. We find, it adsorbs at the top site of the edge position with adsorption energy of -2.21 and 0.04 eV while adsorbed as *CO (Fig. 5a) and *OC (Fig. 5b) structure respectively. The Pt-C and Pt-O bond distances in these structures are 1.94 Å and 2.51 Å respectively. In the bridge position, it

View Article Online
DOI: 10.1039/C5NR01575H

binds through C-atom at the hollow site with adsorption energy of -2.29 eV where the Pt-C bond distance is of 2.11Å (Fig. 5c).

On the other hand, hydrogen adsorbs at the bridge, hollow and top side of Pt(111) facet with adsorption energy of -4.50 eV, -4.33 eV and -4.40 eV respectively.

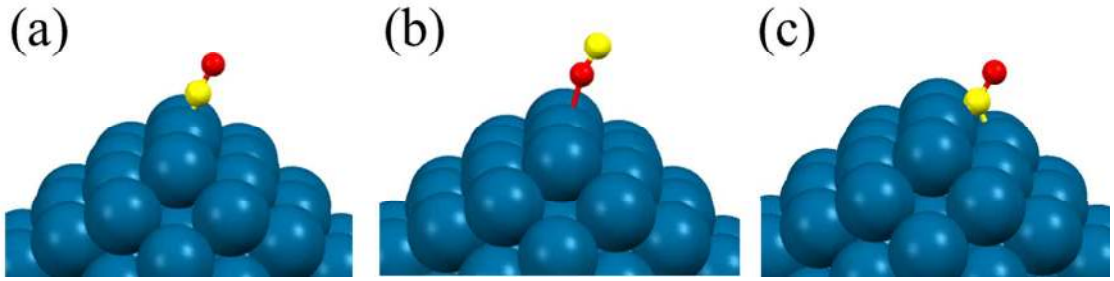

Figure 5: Adsorbed carbon-monoxide at edge via (a) C-atom and (b) O-atom; (c) three-fold hollow

3.4.2. Reaction Energy and Activation Barriers

Carbon monoxide (*CO) can be formed from formyl (*CHO) intermediate via C-H bond activation or from hydroxymethylidyne (*OCH) via O-H bond activation. The possible elementary steps are given as following (steps 9-10 and 9a-10a).

*CHO→ *CO + *H (9) *OCH→ *OC + *H (9a)

*COH→ *CO + *H (10) *OHC→ *OC + *H (10a)

Table 4: Reaction energy (eV) and activation barrier (eV) for the following elementary steps (9-10 and 9a-10a) while adsorbed vertically through C- and O-atom and parallely at the bridge site.

View Article Online
DOI: 10.1039/C5NR01575H

Elementary Reactions	Edge				[1]Bridge	
	[1]C-bonded		[2]O-bonded			
	Reaction Energy	Activation Barrier	Reaction Energy	Activation Barrier	Reaction Energy	Activation Barrier
[1]CHO→ CO + H [2]OCH→ OC + H	-1.00	0.18	-1.50	-	-1.14	0.34
[1]COH→ CO + H [2]OHC→ OC + H	-2.17	0.02	-3.39	-	-0.64	0.52

C-H bond activation

Edge vs. bridge site:

The formation of *CO from formyl is exothermic, irrespective of their binding through C- or O-atom. At the edge position, the C-H bond activation of *CHO calculated to be exothermic by -1.00 eV (step 9) and the barrier is 0.18 eV whereas reaction is exothermic by -1.50 eV when it binds through O-atom (step 9a). We could not locate the TS for the step 9a. In the bridge position, step 9 is calculated to be exothermic by -1.14 eV with the activation barrier of 0.34 eV.

O-H bond activation

Edge vs. bridge site:

The formation of *CO from COH (step 10 and step 10a) via O-H bond activation becomes highly exothermic. Step 10 is exothermic by -2.17 eV with the activation energy of 0.02 eV whereas step 10a is exothermic by -3.39 eV. We could not locate the TS for the step 10a. In the bridge position, step 10 is exothermic by -0.64 eV with the activation energy of 0.52 eV. The formation of *CO at the edge position is more favourable than at the bridge position due

View Article Online
DOI: 10.1039/C5NR01575H

to the little longer O-H bond distance in *COH at the edge position (0.99Å) than at the bridge position (0.98Å).

C-H vs. O-H bond activation:

Our calculated reaction energies and activation barrier study show that at the edge position, the decomposition pathway is more favourable (Scheme 1a) as $*CH_3OH \rightarrow *CH_2OH \rightarrow *CHOH \rightarrow *CHO \rightarrow *CO$ and the reaction steps such as $CH_3OH \rightarrow *CH_3O$, $*CH_2OH \rightarrow *CH_2O$ and $CHOH \rightarrow *COH$ are least favourable.

Similarly, at the bridge position the methanol decomposition is most favourable (Scheme 1c) as $*CH_3OH \rightarrow *CH_2OH \rightarrow *CHOH \rightarrow *COH \rightarrow *CO$ and the reaction steps such as $CH_3OH \rightarrow *CH_3O$, $*CH_2OH \rightarrow *CH_2O$ and $CHOH \rightarrow *CHO$ are last favourable. Therefore in case of edge and bridge position, the difference in the most favoured pathway is in the first and last two steps. The methanol decomposition pathway is not favourable (Scheme 1b) if the intermediates are adsorbed through oxygen centre ($*OHCH_3$).

4. Temperature vs. Rate Constant

To check the effect of temperature on the methanol decomposition reaction, we have calculated the rate constants of the elementary reactions using the following equation

$$k = \frac{k_b T}{h}\left(\frac{P^0}{RT}\right)^{1-n} \exp\left[-\frac{\Delta G_m^{\#}}{RT}\right]$$

where, k and T is the rate constant and reaction temperature and k_b, h, p^0, R, n and ΔG is the Boltzmann's constant, Planck's constant, standard atmospheric pressure and fundamental gas constant, number of reactants and zero-point energy corrected activation barriers respectively.

The methanol decomposition temperature ranges from 323K to 523K, hence the rate constants are calculated at T= 323, 373, 423, 473 and 523K and listed in Table 5-9. It is clear

View Article Online
DOI: 10.1039/C5NR01575H

from the calculated rate constant values that the first two steps of the methanol decomposition reactions proceeds (Table 5-6) very fast when the intermediates are adsorbed parallely in a di-sigma manner. Interestingly, these two steps are reported to be the rate determining steps for the methanol decomposition [17,20,22] and we find if the intermediates are adsorbed in a di-sigma manner then the kinetics of the rate determining steps can be improved significantly. Skoplyak et al. and Peremans et al. reported experimentally that C=O group of methanol interacts paralley to the surface[46] and $-CH_3$ group is also inclined to the surface[47]. Taking into account these experimental observations and our calculated DFT results, we believe methanol molecule and the other dissociated intermediates adsorb in a di-sigma manner which in turns lowers the activation barrier thus increases the catalytic efficiency.

On the other hand, reaction proceeds quite favourable (Table 7-8) at the edge position too and the reaction kinetics are excellent for the last two dehydrogenation steps of the methanol. Our rate constant study could not find any specific step which is slow, so that can be called as a rate determining step which might be due to excellent catalytic activity of the nanocluster. The methanol decomposition is quite slow while proceeds through O-centre (Table 9).

Table 5: Rate of the elementary reactions (s^{-1}) at different temperatures of the most favourable pathway at the bridge position when adsorbs as di-sigma manner.

Elementary Reactions	323K	373K	423K	473K	523K
$CH_3OH \rightarrow CH_2OH\text{-}H$	4.12×10^{11}	9.12×10^{11}	1.73×10^{12}	2.94×10^{12}	4.60×10^{12}
$CH_2OH \rightarrow CHOH\text{-}H$	2.05×10^{13}	2.69×10^{13}	3.42×10^{13}	4.23×10^{13}	$5.^{13}\times10^{13}$
$CHOH \rightarrow COH\text{-}H$	2.73×10^{12}	4.69×10^{12}	7.32×10^{12}	1.07×10^{13}	1.47×10^{13}
$COH \rightarrow CO\text{-}H$	3.61×10^{06}	3.80×10^{07}	2.36×10^{08}	1.02×10^{09}	3.42×10^{09}

Table 6: Rate of the elementary reactions (s^{-1}) at different temperatures of the less favourable pathway at the bridge position when adsorbs as di-sigma manner.

Elementary Reactions	323K	373K	423K	473K	523K
$CH_3OH \rightarrow CH_3O\text{-}H$	1.59×10^{06}	1.87×10^{07}	1.27×10^{08}	5.86×10^{08}	2.07×10^{09}

View Article Online
DOI: 10.1039/C5NR01575H

$CH_3O \rightarrow CH_2O\text{-}H$	5.70×10^{12}	8.97×10^{12}	1.31×10^{13}	1.81×10^{13}	2.40×10^{13}
$CH_2O \rightarrow CHO\text{-}H$	6.37×10^{10}	1.82×10^{11}	4.18×10^{11}	8.26×10^{11}	1.46×10^{12}
$CHO \rightarrow CO\text{-}H$	2.65×10^{08}	1.57×10^{09}	6.29×10^{09}	1.93×10^{10}	4.87×10^{10}

Table 7: Rate of the elementary reactions (s^{-1}) at different temperatures of the most favourable pathway at the edge position when binds through C-atom.

Elementary Reactions	323K	373K	423K	473K	523K
$CH_3OH \rightarrow CH_2OH\text{-}H$	1.69×10^{10}	5.73×10^{10}	1.50×10^{11}	3.30×10^{11}	6.36×10^{11}
$CH_2OH \rightarrow CHOH\text{-}H$	4.99×10^{09}	1.98×10^{10}	5.86×10^{10}	1.41×10^{11}	2.94×10^{11}
$CHOH \rightarrow CHO\text{-}H$	4.06×10^{13}	4.86×10^{13}	5.76×10^{13}	6.74×10^{13}	7.82×10^{13}
$CHO \rightarrow CO\text{-}H$	8.25×10^{11}	1.66×10^{12}	2.94×10^{12}	4.71×10^{12}	7.05×10^{12}

Table 8: Rate of the elementary reactions (s^{-1}) at different temperatures of the less favourable pathway at the edge position when binds through C-atom.

Elementary Reactions	323K	373K	423K	473K	523K
$CH_3OH \rightarrow CH_3O\text{-}H$	4.26×10^{07}	3.21×10^{08}	1.55×10^{09}	5.52×10^{09}	1.57×10^{10}
$CH_3O \rightarrow CH_2O\text{-}H$	1.13×10^{12}	2.18×10^{12}	3.72×10^{12}	5.82×10^{12}	8.52×10^{12}
$CH_2O \rightarrow CHO\text{-}H$	1.55×10^{13}	2.11×10^{13}	2.76×10^{13}	3.50×10^{13}	4.33×10^{13}
$CHO \rightarrow CO\text{-}H$	8.25×10^{11}	1.66×10^{12}	2.94×10^{12}	4.71×10^{12}	7.05×10^{12}

Table 9: Rate of the elementary reactions (s^{-1}) at different temperatures at the edge position when binds through O-atom.

Elementary Reactions	323K	373K	423K	473K	523K
$OHCH_3 \rightarrow H\text{-}OCH_3$	1.16×10^{07}	1.04×10^{08}	5.73×10^{08}	2.26×10^{09}	6.98×10^{09}
$OHCH_3 \rightarrow OHCH_2\text{-}H$	1.00×10^{-05}	3.73×10^{-03}	3.53×10^{-01}	1.31×10^{01}	2.48×10^{02}
$OCH_3 \rightarrow OCH_2\text{-}H$	7.21×10^{13}	7.97×10^{13}	8.88×10^{13}	9.91×10^{13}	1.11×10^{14}
$OHCH_2 \rightarrow OCH_2\text{-}H$	2.63×10^{13}	3.32×10^{13}	4.10×10^{13}	4.97×10^{13}	5.92×10^{13}
$OHCH_2 \rightarrow OHCH\text{-}H$	4.42×10^{-08}	3.47×10^{-05}	5.82×10^{-03}	3.39×10^{-01}	9.27×10^{00}
$OCH_2 \rightarrow OCH\text{-}H$	4.77×10^{-26}	9.49×10^{-21}	1.09×10^{-16}	1.78×10^{-13}	7.18×10^{-11}
$OHCH \rightarrow OCH\text{-}H$	1.30×10^{14}	1.30×10^{14}	1.35×10^{14}	1.42×10^{14}	1.51×10^{14}
$OHCH \rightarrow OHC\text{-}H$	1.69×10^{01}	9.08×10^{02}	1.97×10^{04}	2.28×10^{05}	1.69×10^{06}

View Article Online
DOI: 10.1039/C5NR01575H

5. Conclusion:

DFT calculations have been performed to understand the methanol decomposition pathways on the cuboctahedral platinum nanocluster (Pt_{79}) enclosed by low index facets. Our relative energetic study shows the intermediates adsorbed parallely in a di-sigma manner are the most stable for most of the structures. The calculated reaction energy, activation barriers and temperature dependent reaction constant study shows that methanol decomposition pathway is most favourable at the bridge site while adsorb in a di-sigma manner. Interestingly, the calculated rate constant values show that the first two steps of the methanol decomposition reactions proceeds very fastly when the intermediates are adsorbed parallely in a di-sigma manner. Interestingly, these two steps are reported to be the rate determining steps for the methanol decomposition process and we find the kinetics of the rate determining step can be improved significantly if the intermediates are adsorbed in a di-sigma manner. Our calculated results are compared with previous experimental and theoretical studies and we find our calculated barriers are the lowest when the decomposition is proceeding through a di-sigma manner which is certainly interesting for the methanol dehydrogenation mechanism. To our surprise, methanol experimentally characterized to be adsorbed in a di-sigma manner though no previous theoretical studies consider methanol decomposition mechanism proceeds through a di-sigma manner. Therefore, we believe methanol decomposition might be proceeding through a di-sigma manner.

View Article Online
DOI: 10.1039/C5NR01575H

Acknowledgments:

We thank IIT Indore for the lab and computing facilities. This work is supported by Council of Scientific and Industrial Research [CSIR, Grant number: 01(2723)/13/EMR(II)], New Delhi. A. M. thanks CSIR for the Senior Research Fellowship.

References:

[1] F. Cheng and J. Chen, *Chem. Soc. Rev.,* 2012, **41**, 2172−2192.

[2] B. C. H. Steele and A. Heinzel, *Nature,* 2001, **414**, 345−352.

[3] J. Yang, A. Sudik, C. Wolverton and D. J. Siegel, *Chem. Soc. Rev.,* 2010, **39**, 656−675.

[4] E. Fabbri, D. Pergolesi and E. Traversa, *Chem. Soc. Rev.,* 2010, **39**, 4355−4369.

[5] Y. Wang, K. S. Chen, J. Mishler, S. C. Cho and X. C. Adroher, *Appl. Energy,* 2011, **88**, 981−1007.

[6] H. F. Oetjen, V. M. Schmidt, U. Stimming and F. Trila, *J. Electrochem. Soc.,* 1996, **143**, 3838−3842.

[7] A. Hamnett, *Catal. Today,* 1997, **38**, 445−457.

[8] E. Reddington, A. Sapienza, B. Gurau, R. Viswanathan, S. Sarangapani, E. S. Smotkin and T. E. Mallouk, *Science,* 1998, **280**, 1735−1737.

[9] B. A. Sexton, *Surf. Sci.,* 1981, **102**, 271-281.

[10] D. H. Ehlers, A. Spitzer and H. Luth, *Surf. Sci.,* 1985, **160**, 57-69.

[11] K. D. Gibson and L. H. Dubois, *Surf. Sci.,* 1990, **233**, 59-64.

[12] L. Diekhohner, D. A. Butler, A. Baurichter and A. C. Luntz, *Surf. Sci.,* 1998, **409**, 384-391.

[13] J. W. Peck, D. I. Mahon, D. E. Beck, B. Bansenaur and B. E. Koel, *Surf. Sci.,* 1998, **410**, 214-227.

View Article Online
DOI: 10.1039/C5NR01575H

[14] M. A. Henderson, G. E. Mitchell and J. M. White, *Surf. Sci.,* 1987, **188**, 206-218.

[15] R. J. Levis, Z. C. Jiang, N. Winograd, S. Akhter and K. M. White, *Catal. Lett.,* 1988, 1, 385-389.

[16] J. Wang and R. I. Masel, *J. Am. Chem. Soc.,* 1991, **113**, 5850-5856.

[17] J. Greeley and M. Mavrikakis, *J. Am. Chem. Soc.,* 2002, **124**, 7193-7201.

[18] Y. Ishikawa, M. S. Liao and C. R. Cabrera, *Sur. Sci.,* 2000, **463**, 66–80.

[19] S. K. Desai, M. Neurock and K. Kourtakis, *J. Phy. Chem. B,* 2002, **106**, 2559–2568.

[20] C. Y. Niu, J. Jiao, B. Xing, G. C. Wang and X. H. Bu, *J. Comp. Chem.,* 2010, **31**, 2023–2037.

[21] N. Tian, Z. Zhou, S. Sun, Y. Ding and Z. L. Wang, *Science,* 2007**, 316***,* 732-735.

[22] J. Greeley and M. Mavrikakis, *J. Am. Chem. Soc.,* 2004, **126**, 3910-3919.

[23] N. Tian, Z. Zhou and S. Sun, *J. Phys. Chem. C,* 2008**, 112***,* 19801–19817.

[24] J. Kua and W. A. Goddard, *J. Am. Chem. Soc.,* 1999, **121**, 10928-10941.

[25] S. Dobrin, *Phys. Chem. Chem. Phys.,* 2012, **14***,* 12122-12129.

[26] I. V. Yudanov, A. Genest and N. *J.* Rösch, *Cluster Sci.,* 2011, **22**, 433-448.

[27] I. V. Yudanov, A. Genest, S. Schauermann, H. J. Freund and N. Rösch, *Nano Lett.,* 2012, **12**, 2134-2139.

[28] L. Li, A. H. Larsen, N. A. Romero, V. A. Morozov, C. Glinsvad, F. A. Pedersen, J. Greeley, K. W. Jacobsen and J. K. Nørskov, *J. Phys. Chem. Lett.,* 2013, **4**, 222-226.

[29] N. Lopez, T. V. W. Janssens, B. S. Clausen, Y. Xu, M. Mavrikakis, T. Bligaard and J. K. Nørskov, *J. Catal.,* 2004, **223**, 232-235.

[30] L. M. Molina and B. Hammer, *Appl. Catal. A,* 2005, **291**, 21-31.

[31] J. Greeley, J. K. Nørskov and M. Mavrikakis, *Annu. Rev. Phys. Chem.,* 2002, **53**, 319-348.

[32] B. Hammer and J. K. Nørskov, *Surf. Sci.,* 1995**, 343**, 211-220.

View Article Online
DOI: 10.1039/C5NR01575H

[33] B. Z hang, D. Wang, Y. Hou, S. Yang, X. H. Yang, J. H. Zhong, J. Liu, H. F. Wang, P. Hu, H. J. Zhao and H. G. Yang, *Sci. Rep.,* 2013, **3**, 1836

[34] Y. Hu, H. Zhang, P. Wu, H. Zhang, B. Zhou and C. Cai, *Phys. Chem. Chem. Phys.,* 2011, **13**, 4083-4094.

[35] T. Maiyalagan, F. N. Khan, *Catal. Comm.,* 2009, **10**, 433-436.

[36] H. Ha, I. Y. Kim, S. Hwang and R. S. Ruoff, *Electrochem. Solid State Lett.* 2011, **14**, B70-B73.

[37] L. Xiong and A. Manthiram *J. Electrochem. Soc.,* 2005, **152**, A697-A703.

[38] P. E. Blochl, *Phy. Rev. B,* 1994, **50**, 17953-17979.

[39] (a) G. Kresse and J. Hafner, *Phy. Rev. B,* 1993, **47**, 558-561. (b) G. Kresse and J. Hafner, *Phy. Rev. B,* 1994, **49**, 14251-14269. (c) G. Kresse and D. Joubert, *Phy. Rev. B,* 1999, **59**, 1758-1775.

[40] J. P. Perdew, J. A. Chevary, S. H. Vosko, K. A. Jackson, M. R. Pederson, D. J. Singh and C. Fiolhais, *Phy. Rev. B,* 1992, **46**, 6671-6687.

[41] G. Henkelman and H. Jonsson, *J. Chem. Phys.,* 2000, **113**, 9978-9985.

[42] E. Shustorovich, *Adv. Catal.,* 1990, **37** 101-163.

[43] Z. C. Kramer, X. Gu, D. D. Y. Zhou, W. Li and R. T. Skodje, *J. Phys. Chem. C,* 2014, **118**, 12364-12383.

[44] C. Zheng, Y. Apeloig and R. Hoffmann, *J. Am. Chem. Soc.,* 1988**, 110** 749-774.

[45] J. R. B. Gomes and J. A. N. F. Gomes, *J. Electronanal. Chem.,* 2000, **483**, 180-187.

[46] O. Skoplyak, C. A. Menning, M. A. Barteau and J. G. Chen, *J. Chem. Phys.,* 2007, **127**, 114707.

[47] A. Peremans, J. Maseri, J. Darville and J. M. Gilles, *Sur. Sci.,* 1990**, 227***,* 73-78.

View Article Online
DOI: 10.1039/C5NR01575H

Table of Content